

Protein phosphatase 2A promotes hepatocellular carcinogenesis in the diethylnitrosamine mouse model through inhibition of p53

François H.T.Duong¹, Michael T.Dill^{1,2}, Matthias S.Matter³, Zuzanna Makowska¹, Diego Calabrese¹, Tanja Dietsche³, Sylvia Ketterer¹, Luigi Terracciano³ and Markus H.Heim^{1,2,*}

¹Department of Biomedicine and ²Division of Gastroenterology and Hepatology, University Hospital Basel, CH-4031 Basel, Switzerland and ³Department of Molecular Pathology, Institute for Pathology, University Hospital Basel, CH-4003 Basel, Switzerland

*To whom correspondence should be addressed. Division of Gastroenterology and Hepatology, University Hospital Basel, Petersgraben 4, CH-4031 Basel, Switzerland. Tel: +41 61 265 33 62; Fax: +41 61 265 53 52; Email: markus.heim@unibas.ch

Hepatocellular carcinoma (HCC) is one of the most common cancers worldwide. Most HCCs develop in cirrhotic livers. Alcoholic liver disease, chronic hepatitis B and chronic hepatitis C are the most common underlying liver diseases. Hepatitis C virus (HCV)-specific mechanisms that contribute to HCC are presently unknown. Transgenic expression of HCV proteins in the mouse liver induces an overexpression of the protein phosphatase 2A catalytic subunit (PP2Ac). We have previously reported that HCV-induced PP2Ac overexpression modulates histone methylation and acetylation and inhibits DNA damage repair. In this study, we analyze tumor formation and gene expression using HCV transgenic mice that overexpress PP2Ac and liver tissues from patients with HCC. We demonstrate that PP2Ac overexpression interferes with p53-induced apoptosis. Injection of the carcinogen, diethylnitrosamine, induced significantly more and larger liver tumors in HCV transgenic mice that overexpress PP2Ac compared with control mice. In human liver biopsies from patients with HCC, PP2Ac expression was significantly higher in HCC tissue compared with non-tumorous liver tissue from the same patients. Our findings demonstrate an important role of PP2Ac overexpression in liver carcinogenesis and provide insights into the molecular pathogenesis of HCV-induced HCC.

Introduction

Hepatocellular carcinoma (HCC) is the most prevalent primary liver cancer and a major cause of cancer mortality worldwide. The major risk factor for HCC is chronic hepatitis B, followed by chronic hepatitis C (CHC) and chronic alcoholic liver disease (1). In Europe, most HCCs occur in cirrhosis, and it is well established that cirrhosis is a major risk factor for HCC independent of the underlying liver disease. However, in the context of chronic hepatitis B or CHC, HCC can develop also in non-cirrhotic livers. Virus-induced chronic inflammation can impair DNA damaged repair, rendering cells more susceptible to spontaneous or mutagen-induced alterations (2). There are also experimental evidences of the oncogenic potential of hepatitis C virus (HCV) proteins such as HCV core. For instance, it has been reported that HCV core transgenic mice develop hepatic steatosis and HCC at the age of 16–19 months (3).

We have reported previously that HCV infection induces an upregulation of protein phosphatase 2A (PP2A) catalytic subunit through an endoplasmic reticulum stress response pathway (4,5). PP2A is a heterotrimeric protein phosphatase consisting of a 36 kD catalytic C subunit (PP2Ac), a 65 kD structural A subunit and a variable

Abbreviations: CHC, chronic hepatitis C; CREB, cyclic adenosine monophosphate response element-binding protein; DEN, diethylnitrosamine; HCC, hepatocellular carcinoma; HCV, hepatitis C virus; PP2Ac, protein phosphatase 2A catalytic subunit; SEM, standard error of the mean.

regulatory B subunit. This phosphatase is widely expressed in all cell types and is involved in the posttranslational control of signaling proteins by performing reversible phosphorylation (6). In recent work, we observed that HCV-induced PP2Ac overexpression in cells leads to an inhibition of histone H4 posttranslational modifications and impairs the DNA repair machinery (7). We also found that cotransfection of c-myc and HA-PP2Ac plasmids into NIH3T3 cells significantly increased c-myc-induced anchorage-independent growth. These data suggested that PP2Ac overexpression may contribute to hepatocellular carcinogenesis in the context of CHC.

Cells are constantly exposed to DNA damage. In order to prevent the propagation of mutations, cells have evolved systems that sense DNA damage and interrupt the cell cycle to allow repair of damaged DNA. If DNA damage is too severe and irreparable, cells undergo apoptosis (8). DNA damage is a hallmark of cancer cells. DNA damage repair is often ineffective and proapoptotic pathways are non-functional in many cancer types, resulting in an accumulation of mutations during cancer evolution (9). PP2A is of particular interest in the control of apoptotic networks because of its predominant tumor-suppressive characteristics (10). However, some reports have shown that particular PP2A complexes can counterbalance the apoptotic cell death program as well. Indeed, it has been described that cyclin G associates with PP2A holoenzyme containing B' subunits and directs the phosphatase complex to the murine double minute 2 (Mdm2), where PP2A dephosphorylates Mdm2 on threonine 216, leading to a negative regulation of p53 apoptotic function (11).

The tumor suppressor protein p53 can initiate cell cycle arrest, DNA repair and apoptosis (12,13). In resting cells, constant degradation through the proteasome pathway maintains low expression levels of p53. Upon DNA damage, p53 is stabilized and accumulated (14). This stabilization results from phosphorylation of p53 on serine 15 within the transactivation domain, inhibiting the association to Mdm2, thereby preventing p53 ubiquitination and proteasomal degradation (15). Several functions of p53 are also regulated by phosphorylation (16,17). For instance, phosphorylation of p53 on serine 37 and 46 is associated with induction of transcriptional activity and apoptosis (18,19). p53 is frequently found to be mutated in human cancer (20,21), and malignancies that retain a wild-type p53 gene usually acquire other impairments that affect p53 function (22), suggesting that p53 inactivation is a common step in most human cancers development.

In this study, we investigated p53 modifications and apoptotic pathways in PP2Ac-overexpressing cells and HCVcc-infected cells. We show that PP2Ac overexpression reduces p53 phosphorylation in response to DNA-damaging agents. Consequently, expression of p53 proapoptotic genes is reduced, and apoptosis is inhibited. HCV transgenic mice that overexpress PP2Ac were more susceptible to diethylnitrosamine (DEN) and had more and larger liver tumors. In human liver biopsies from patients with CHC and HCC, we found an overexpression of PP2Ac in tumor tissue and observed a significant negative correlation between PP2Ac and PUMA/Noxa expression.

Materials and methods

Cells and reagents

UHC57.3, HA-PP2Ac and short-hairpin small interfering RNA PP2Ac cells were described previously (4,7,23). Etoposide and DEN were purchased from Sigma-Aldrich (Fluka Chemie GmbH, Buchs, Switzerland). Etoposide was obtained from Bristol-Myers Squibb SA (Baar, Switzerland). Anti-HCV core (clone C7-50) was from ABR Affinity Bioreagents (Lucerne Chem AG, Lucerne, Switzerland). Anti-Caspase-9, cleaved Caspase-3, pSer15p53, pSer37p53, pSer18p53 and pSer46p53 were from Cell Signaling (Bioconcept, Allschwil, Switzerland). Anti-PP2Ac was from Millipore AG (Zug, Switzerland). Anti-p53 was from Santa Cruz Biotechnology (LabForce AG, Nunningen, Switzerland).

HCV particles production and infection of Huh7.5.1 cells

RNA preparation and electroporation were done as described (24). Huh7.5.1 cells were infected with HCV particles at multiplicity of infection of 1 for 3 days.

Animals and experimental design

HCV transgenic mice (B6HCV) were described previously (25). The DEN injection study was performed in two groups of mice: C57BL6 injected with DEN (5 µg/g) ($n = 22$) and B6HCV injected with DEN (5 µg/g) ($n = 19$). DEN was injected once intraperitoneally to mice at 2 weeks of age. The animals were euthanized 40 weeks after injection by CO₂ inhalation. The resected liver lobes were immediately frozen in liquid nitrogen and kept at -70°C. The Etopophos injection study was performed in four groups of mice at 8 weeks of age: C57BL6, no injection ($n = 2$); C57BL6 injected with Etopophos (100 mg/m²) ($n = 2$); B6HCV, no injection ($n = 2$) and B6HCV injected with Etopophos (100 mg/m²) ($n = 2$). Etopophos was injected intraperitoneally to the mice and the animals were euthanized after 2 h.

Microcystin LR (Sigma–Aldrich, Fluka Chemie GmbH) injection (70 µg/kg) was performed intraperitoneally, and the mice were euthanized after 2 h.

Protein preparation and western blotting analysis

Whole cell extracts (from cell lines and from mouse liver tissues) and western blot analysis were performed as described previously (7,26). Densitometry analysis of protein bands was performed with ImageJ software (NIH Image).

RNA isolation, reverse transcription and SYBR–PCR

RNA isolation, reverse transcription and SYBR–PCR were done as described previously (7). The human primers were 5'-TCTTCCTCTGAGGCGAGCT-3' and 5'-AGGTGTGTGTCTGAGCCC-3' for *p53AIP1*; 5'-AGAGCTGGAA GTCGAGTGT-3' and 5'-GCACCTTCACATTCCTCTC-3' for *Noxa*; 5'-AAG ACCATGTGGACCTGT-3' and 5'-GGTAGAAATCTGTATGCTG-3' for *p21*; 5'-CCTGCCAGATTTGTGAGACAAG-3' and 5'-CAGGAGTCCCATGATG AGATTG-3' for *PUMA*; 5'-CCACAGCAAGTCACACATTGG-3' and 5'-CAG AGCACTTGATCGCCTACAA-3' for *PP2Ac*; 5'-GCTCTCCTGTTTCGACA GTCA-3' and 5'-ACCTTCCCCATGGTGTCTGA-3' for *GAPDH*. The mouse primers were 5'-ATCCGCAAGCCTGTGACTGT-3' and 5'-TCGGGCCAGG GTGTTTTT-3' for *RPL19*; 5'-GCCAGCAGCACTTAGAGTC-3' and 5'-TGT CGATGCTGCTCTTCTTG-3' for *PUMA*; 5'-CCCAGATTGGGGACCTTA GT-3' and 5'-TCCTCATCTGCTCTTTTGC-3' for *Noxa*.

Paired liver biopsies

All patients were recruited in the Hepatology Outpatient Clinic of the University Hospital Basel, Switzerland. All patients gave written informed consent to participate in this study and donated a liver biopsy specimen for research purposes. The study was approved by the Ethics Committee of Basel.

Biopsies of the tumor and non-tumorous tissue from a distal site of the liver were performed using coaxial technique. One biopsy specimen from each site was assessed by a pathologist. Biopsy specimens with at least 50% of HCC tissue in the tumor sample and tumor free in the control sample were used for the analysis.

Biopsy samples were frozen immediately after collection and stored in liquid nitrogen until processing. Total RNA was extracted using Qiazol reagent and RNeasy Mini Kit (Qiagen) according to the manufacturer's instructions. Reverse transcription and quantitative PCR were performed as described above.

Soft agar assay

Human hepatoma cells and human primary lung fibroblasts (kindly provided by Prof. Michael Roth) transfected with HA-PP2Ac plasmid using FuGene HD, according to the manufacturer's recommendations, were cultured for 7 days in a semisolid culture media, and colonies were visualized under light microscopy.

Caspase-9 assay

Huh7 and HA-PP2Ac cells were treated with 100 µM etoposide for 1 h, and caspase-9 activity was measured using Caspase-Glo 9 Assay (Promega AG, Dübendorf, Switzerland) according to the manufacturer's instructions.

In vitro dephosphorylation assay

Whole cell lysate from Huh7 cells stimulated with 100 µM etoposide for 1 h was prepared and then incubated with or without 1 U of purified PP2A (Upstate, Millipore AG) at 37°C for 10 min. The reaction was then stopped by heating at 100°C for 5 min and then loaded on a sodium dodecyl sulfate–polyacrylamide gel electrophoresis. pSer15p53, pSer37p53 and pSer46p53 were then visualized with specific antibodies.

Cleaved caspase-3 immunofluorescence staining

Briefly, sections (10 µm) from mouse liver embedded in optimal cutting temperature compound were prepared and mounted onto polylysine slides (Thermo Fisher Scientific, Wohlen, Switzerland). Tissue sections were then fixed in absolute methanol (-20°C, 15 min) and then rinsed twice in phosphate-buffered saline before being blocked in a 2% bovine serum albumin and 0.2% Triton-X solution for 30 min at room temperature. Primary antibody incubation was performed overnight at 4°C. Slides were then rinsed twice in phosphate-buffered saline. Epitopes detection was performed using fluorescein-conjugated goat anti-rabbit (Invitrogen Molecular Probes, Eugene, OR). Nuclei were stained by 4',6-diamidino-2-phenylindole, and slides were mounted with a water-based mounting medium (Ultramount Aqueous Permanent Mounting Medium; Dako, Carpinteria, CA).

Paraffin-embedded sections and hematoxylin staining

Fresh liver tissue was fixed in 4% paraformaldehyde overnight. Afterwards, tissue was embedded in paraffin, and the sections of 4 µm thickness were prepared, stained with H&E and analyzed under light microscopy. Liver tumors were classified according to a consensus report on murine liver lesions (27).

Results

PP2Ac overexpression impairs p53 phosphorylation, p53-induced target genes expression and p53-induced apoptosis

We have shown previously that the expression of HCV proteins in cells induces PP2Ac protein expression (4). To explore a potential role of PP2A in the regulation of p53 function, we used cells that allow the inducible expression of HCV proteins (UHCV57.3 cells) to upregulate PP2Ac and then stimulated p53 phosphorylation with the DNA-damaging agent etoposide. As shown in Figure 1, HCV-mediated upregulation of PP2Ac impaired etoposide-induced p53 phosphorylation on serine 37 and 46 (Figure 1A) and significantly reduced expression of the canonical p53 target genes—*p53AIP1*, *Noxa*, *p21* and *PUMA* (Figure 1B). Next, we confirmed the role of PP2Ac in Huh7-derived cells that express a constitutive active form of PP2Ac (HA-PP2Ac). Compared with control Huh7 cells, etoposide-induced phosphorylation of serine 37 and 46 was significantly inhibited (Figure 1C). Accordingly, the induction of p53 target genes was also reduced in HA-PP2Ac (Figure 1D).

There was also a slight reduction of serine 15 phosphorylation in UHCV57.3 cells but not in HA-PP2Ac cells. To assess if HCV causes an additional inhibition of p53 phosphorylation on serine 15, we infected Huh7.5 cells with the cell culture infectious JC-1 clone of HCV. HCV-infected cells indeed had an overexpression of PP2Ac, and etoposide-induced phosphorylation of serine 37 and 46 was inhibited (Supplementary Figure S1, available at *Carcinogenesis* Online). However, no change in serine 15 phosphorylation was observed.

We further explored the mechanism by which PP2A reduces etoposide-induced p53 phosphorylation using an *in vitro* dephosphorylation assay. Extracts from etoposide-treated Huh7 cells were incubated with purified PP2A for 10 min, followed by western blotting using antibodies specific for phosphorylated serine residues on p53. There was a strong reduction of phosphoserine 37 and 46 but no effect on serine 15 (Supplementary Figure S2, available at *Carcinogenesis* Online).

Activated p53 can eliminate tumor cells by inducing apoptosis through caspase-9 activation. We, therefore, measured caspase-9 activity following etoposide treatment and found that the activity of caspase-9 was significantly reduced in HA-PP2Ac cells compared with Huh7 cells (Figure 2A), suggesting that PP2Ac overexpression could favor the survival of transformed cells. Next, we transfected human primary lung fibroblasts with the HA-PP2Ac plasmid and performed a cell anchorage-independent growth assay. In line with our data that were published previously (7), PP2Ac overexpression resulted in transformation of human primary lung fibroblasts as illustrated by colony formation in soft agar media (Figure 2B).

The role of PP2A in the regulation of p53 function was further explored by silencing PP2Ac using short-hairpin small interfering RNA. Knockdown of PP2Ac resulted in an increased

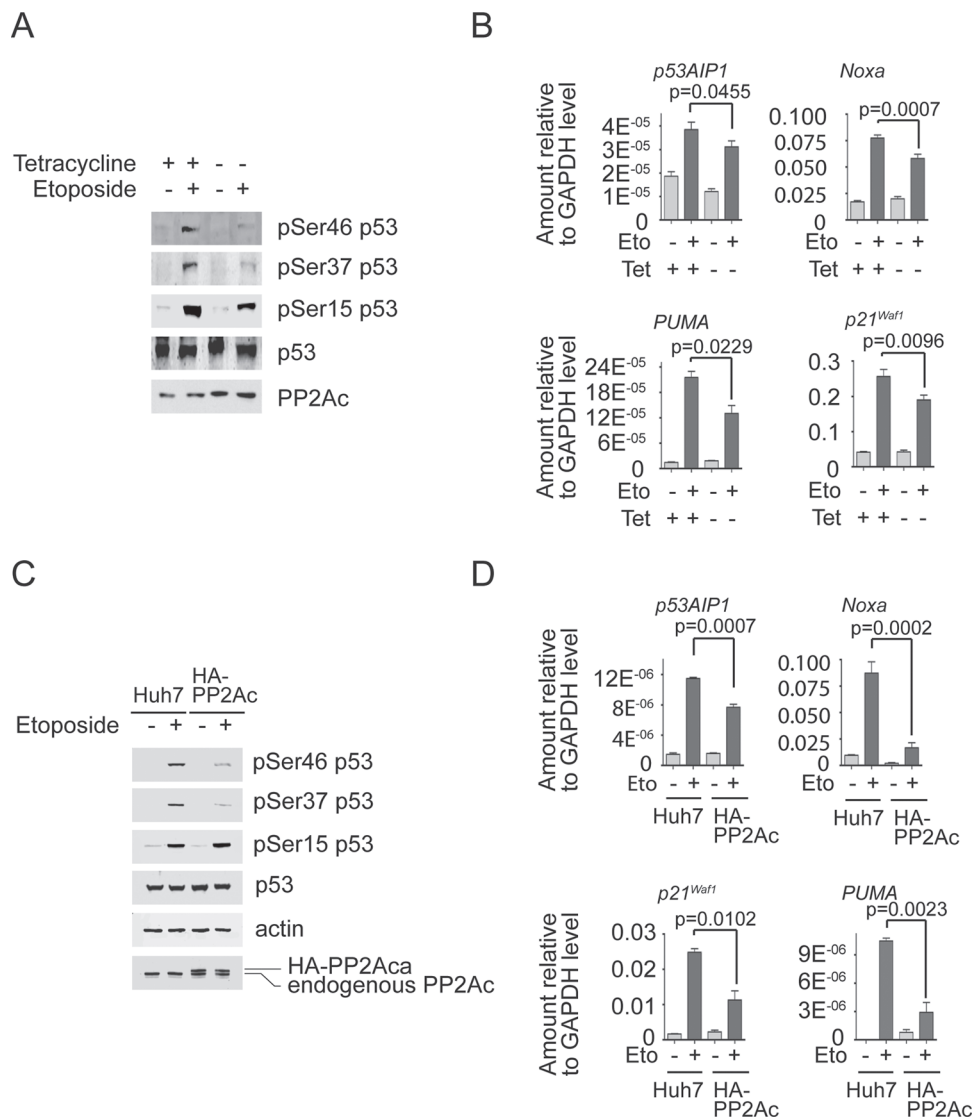


Fig. 1. PP2Ac overexpression impairs p53 phosphorylation and expression of p53 proapoptotic genes. (A) UHCV57.3 cells were derepressed by tetracycline for 24 h in order to induce the expression of HCV proteins. Cells were then exposed to 100 μ M etoposide for 1 h, and phosphorylation of p53 on serine 15, 37 and 46 was analyzed by western blotting. (B) Cells were stimulated with 100 μ M etoposide for 24 h, and total RNA was isolated and reverse transcribed to complementary DNA. The expression of genes was measured by quantitative PCR (qPCR). Results are expressed as mean \pm standard error of the mean (SEM) from three independent experiments. Statistical analysis was performed using Student's *t*-test. (C) Huh7 and HA-PP2Ac cells were exposed to 100 μ M etoposide for 1 h, and phosphorylation of p53 on serine 15, 37 and 46 was analyzed by western blotting. (D) Huh7 and HA-PP2Ac cells were exposed to 100 μ M etoposide for 24 h, and RNA was isolated. The expression of genes was monitored by qPCR. Results are expressed as mean \pm SEM from three independent experiments.

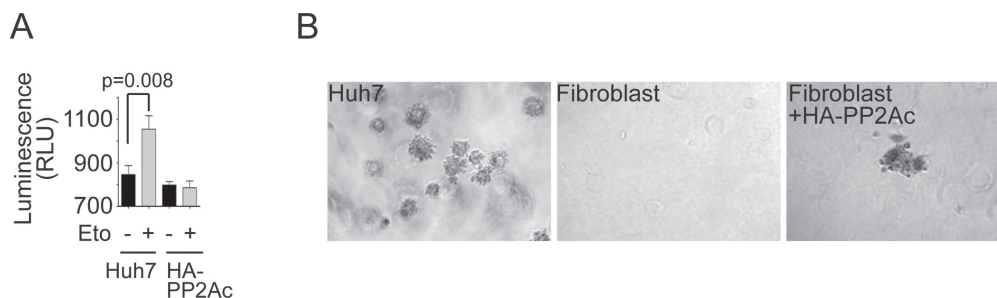


Fig. 2. PP2Ac overexpression reduces caspase-9 activation upon etoposide stimulation and promotes fibroblast transformation. (A) Huh7 and HA-PP2Ac cells were stimulated with 100 μ M etoposide for 1 h, and caspase-9 activity was measured using Caspase-Glo 9 Assay. Results are expressed as mean \pm SEM from two independent experiments. (B) Huh7 cells or human fibroblasts untransfected or transfected with an HA-PP2Ac coding plasmid were cultured on a semisolid culture media for 7 days. Colonies were visualized by light microscopy. Representative pictures of colonies after 7 days of culture on semisolid support are shown.

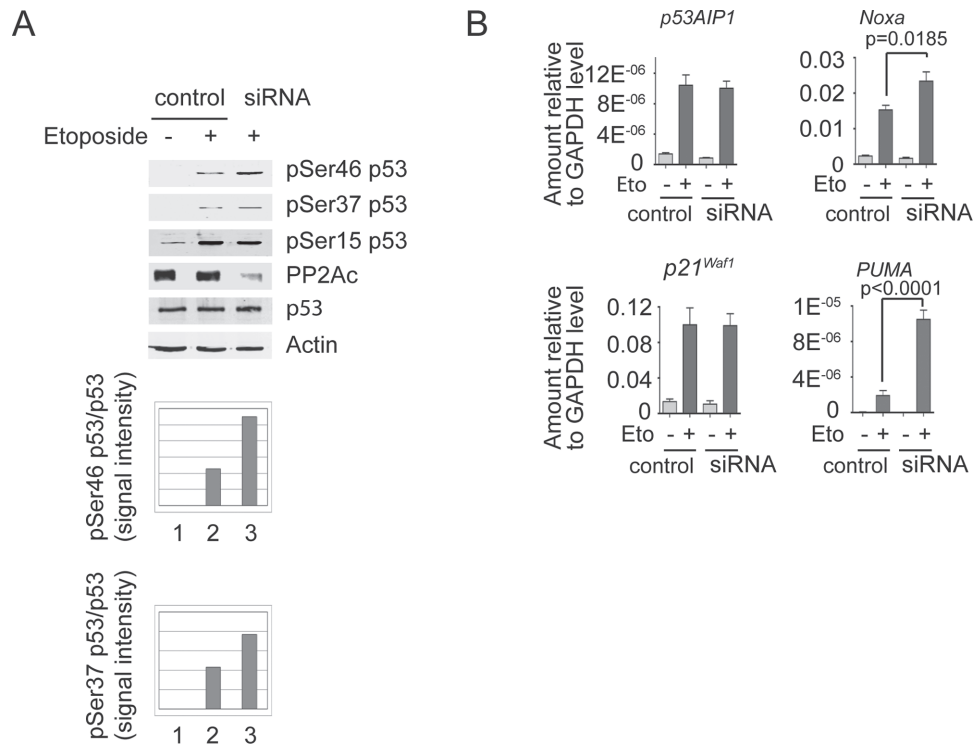


Fig. 3. PP2Ac silencing alters p53 phosphorylation and p53-induced proapoptotic genes expression. (A) Control-scrambled and short-hairpin small interfering RNA PP2Ac cells were treated with 100 μ M etoposide for 1 h, and phosphorylation on p53 was monitored by western blotting. A representative blot from at least two independent experiments is shown. (B) Cells were treated with 100 μ M etoposide for 24 h, and the expression of the genes was quantified by quantitative PCR. Results are expressed as mean \pm SEM from three independent experiments.

etoposide-induced phosphorylation of p53 on serine 37 and 46, but not on serine 15 (Figure 3A), and consequently a significantly higher expression of *Noxa* and *PUMA*, two direct p53-induced apoptotic genes (Figure 3B).

PP2Ac overexpression in B6HCV mice impairs Ettophos-mediated p53 phosphorylation, reduces DEN-induced p53 target gene expression and increases DEN-induced HCC formation

To assess the *in vivo* relevance of our findings, we injected B6HCV and C57BL6 control mice with Ettophos. We used B6HCV mice because no transgenic mouse model with direct PP2Ac overexpression exists, but B6HCV mice consistently showed a significant overexpression of PP2Ac in the liver (4). Upon Ettophos injection, we observed phosphorylation of p53 on serine 18 (homologue to serine 15 in human) in liver homogenates of C57BL6 mice. This phosphorylation is impaired in B6HCV mice (Figure 4A). We were not able to investigate phosphorylation on serine 46 and 37 because no antibodies against these phosphorylation sites are available for mouse. We investigated further the effect of PP2A on p53-mediated apoptosis by analyzing caspase-9 cleavage upon injection with microcystin LR, a DNA damage compound. As shown in Supplementary Figure S3, available at *Carcinogenesis* Online, a clear reduction of cleaved caspase-9 in B6HCV mice can be observed, suggesting a reduction of apoptosis in these transgenic animals.

Carcinogenesis is a complex process involving alterations of DNA damage repair and apoptosis (28). We have shown previously that PP2Ac overexpression renders cells more susceptible to DNA damage and impairs DNA repair (7). In the present paper, we report an impairment of apoptosis. We, therefore, investigated if B6HCV mice that overexpress PP2Ac are more susceptible to HCC. B6HCV and C57BL6 mice were injected with DEN, a carcinogen known to induce liver tumors in mice. Mice were euthanized 40 weeks after a single injection of a low dose of DEN. We observed a reduction of *Noxa* and *PUMA*, two direct p53 target genes (Figure 5A) in non-tumoral liver tissue obtained from B6HCV mice, suggesting a diminution of p53

proapoptotic function. We, therefore, analyzed cleaved caspase-3 in B6HCV and in C57BL6 mice. Our data show a reduction of caspase-3 cleavage in B6HCV mice compared with control animals, suggesting a diminution of DEN-induced apoptosis in the transgenic mice (Figure 5B). We confirmed these results by staining cleaved caspase-3 on liver sections. As shown in Figure 5C, C57BL6 mice showed more caspase-3 cleavage than B6HCV mice. Furthermore, we observed pronounced chromatin condensation in control animals compared

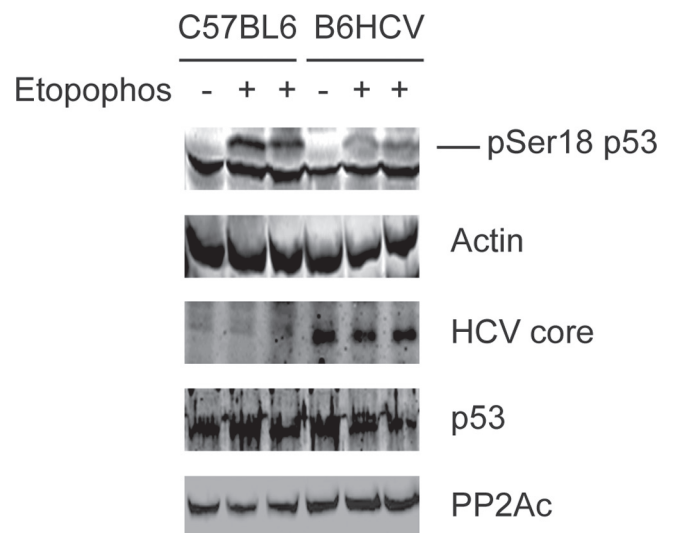


Fig. 4. PP2Ac overexpression in HCV transgenic mice impairs p53 phosphorylation upon Ettophos injection. Eight-week-old C57BL6 ($n = 2$) and B6HCV ($n = 2$) mice were injected with Ettophos and killed 2 h later. Liver homogenates were analyzed by western blotting with antibodies to phosphoserine 18 on p53, p53, actin, HCV core and PP2Ac.

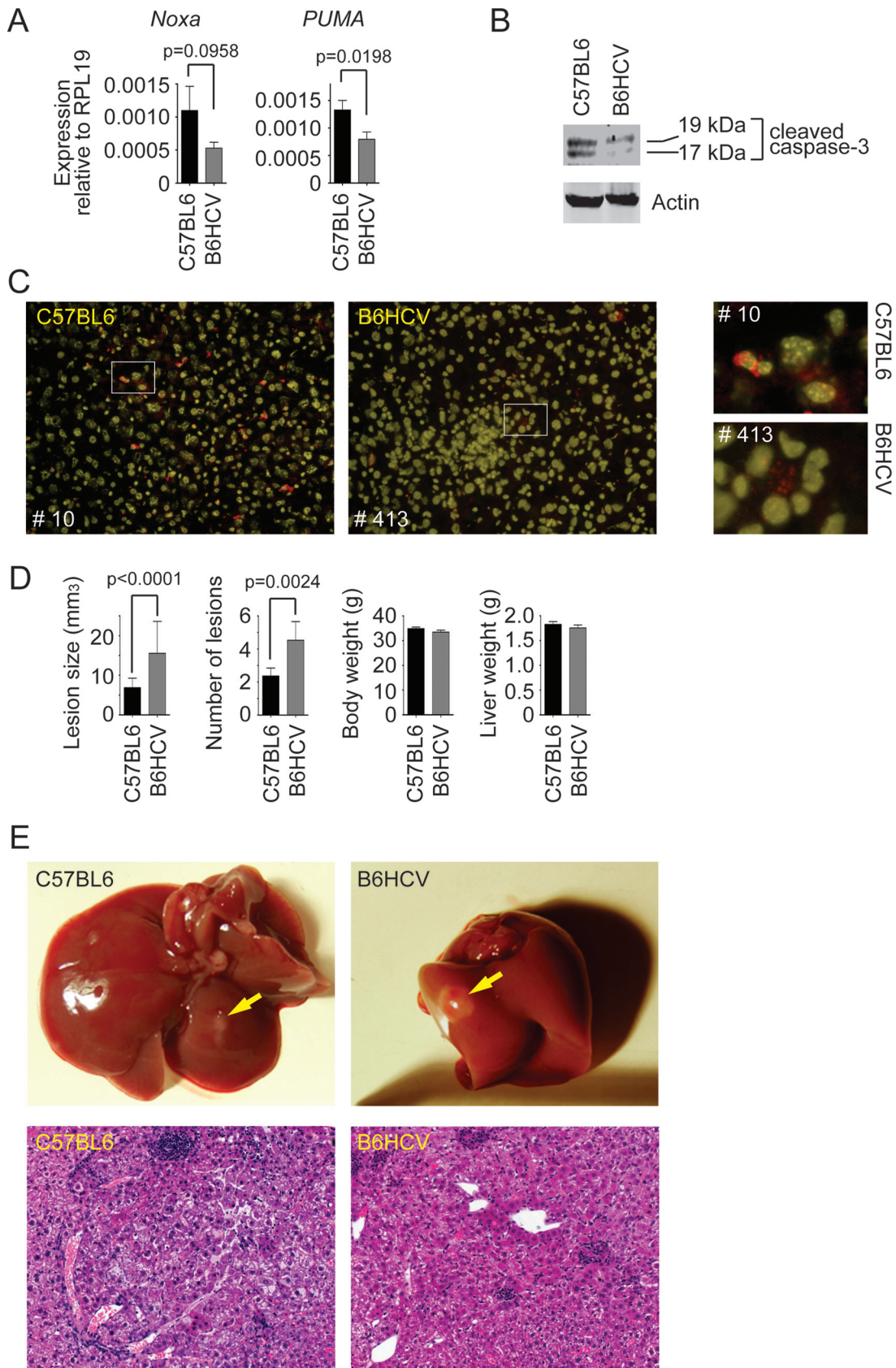


Fig. 5. PP2Ac overexpression in HCV transgenic mice reduces p53 proapoptotic function and enhances liver tumor formation upon DEN injection. (A) C57BL6 and B6HCV mice were injected intraperitoneally with DEN at 5 µg/g of body weight. Animals were killed 40 weeks after DEN administration. The expression of *Noxa* and *PUMA* was quantified by quantitative PCR and expressed relative to *RPL19*. Results are expressed as mean ± SEM from 22 control animals and 17 transgenic mice, and statistical analysis was performed using Student's *t*-test. (B) Cleaved caspase-3 was detected by immunoblotting in liver homogenates from mice injected with DEN. A representative blot is shown. (C) Detection of caspase-3 cleavage by immunofluorescence from mouse liver sections. A representative

with transgenic mice, demonstrating more apoptosis in C57BL6 mice (Figure 5C). We counted more liver tumors in B6HCV mice than in C57BL6 mice (Figure 5D). These liver tumors were bigger in B6HCV mice than in control mice (Figure 5D and 5E). The body weight and the liver weight remained unchanged between control and transgenic mice (Figure 5D). Histology of the liver tumors did not show any significant difference between B6HCV and C57BL6 mice (Figure 5E). In both groups, the tumors were characterized by loss of the normal lobular architecture and displayed irregular growth pattern. They were sharply demarcated from the surrounding liver parenchyma that was often compressed. Moreover, focal areas of cellular atypia characterized by slight pleomorphic nuclei, coarsely clumped chromatin, large nucleoli and cytoplasmic basophilia were

also present. All these histological features are consistent with murine hepatocellular adenomas, which are typically found after a single DEN injection (29).

PP2Ac is upregulated in tumorous liver biopsies and negatively correlated with p53 proapoptotic gene expression

In order to assess the correlation between PP2Ac expression and p53 proapoptotic gene expression in humans, we performed a quantitative PCR analysis using paired liver biopsies from HCC and from tissue outside the tumors collected from patients with and without CHC (Table I). Indeed, analysis of PP2Ac expression revealed a higher expression of PP2Ac in malignant tissue than in non-tumorous surrounding tissue both from non-CHC patients (Figure 6A). We then

Table I. Clinical characteristics of HCC liver biopsies

No.	Code	Age	Sex	Fibrosis grade	HCV/HBV infection	Alcohol abuse	Focality	Pathology	Edmonson grade
1	A1	63	M	F4	No virus	Yes	Multifocal	Trabecular, pseudoglandular, inflammation	III
2	A12	69	M	F0	No virus	No	Singular	Trabecular, focally necrotic	II
3	A37	68	M	F4	No virus	Yes	Singular	Trabecular-sinusoidal	II
4	A255	79	F	F3–F4	HBV	No	Singular	Trabecular	II
5	A268	63	M	F4	No virus	Yes	Multifocal	Trabecular, hyaline globules	II
6	A286	63	M	F3	No virus	–	Singular	Trabecular, lamellar fibrosis, steatosis	II
7	A367	64	M	F3–F4	No virus	Yes	Singular	Trabecular, focally clear cell	II
8	A442	75	M	F4	No virus	Yes	Multifocal	NA	II
9	A722	80	F	F1	HCV GT NA	No	Singular	Trabecular	II
10	A724	60	M	F4	HBV	No	Multifocal	Mixed hepatocholangiocarcinoma	III
11	A824	62	M	F3–F4	HBV	Yes	Singular	Mixed hepatocholangiocarcinoma	III
12	A829c	30	M	F1–F2	HBV	No	Singular	Stem cell-like, mixed hepatocholangiocarcinoma	IV
13	A835	56	M	F4	HCV GT 3a	Yes	Three nodules	Trabecular, steatosis, desmoplastic	III
14	A879	67	M	F3–F4	HBV	–	Multifocal	Trabecular	II
15	A896	71	M	F4	No virus	Yes	Multifocal	Trabecular	III
16	A911	52	M	F4	HCV GT NA	–	NA	Pseudoglandular	II
17	A915	85	M	F0–F1	No virus	No	Singular	Trabecular, pseudoglandular	II
18	A941	48	M	F4	HCV GT 1a (6.25 log10)	Yes	Multifocal	Trabecular, partly necrotic	III
19	A969	68	M	F4	No virus	No	Singular	Trabecular	II
20	B21	75	M	F4	No virus	Yes	Singular	Trabecular, Mallory bodies, granulomatous inflammation	II–III
21	B39	59	M	F4	No virus	Yes	Singular	Trabecular, inflammation	III
22	B62	58	F	F4	HBV	–	Singular	Trabecular	II (focally I)
23	B77	59	M	F4	No virus	Yes	Multifocal	Solid	III
24	B156	78	M	F4	No virus	Yes	Multifocal	Trabecular, microacinary	II
25	B214a	75	M	F3	No virus	Yes	Two foci	Solid	II
26	B277	62	M	F4	HCV GT 1b (4.79 log10)	–	Singular	Solid, necrosis, inflammation	III
27	B313	69	F	F4	HBV	No	Two foci	Trabecular, inflammation	II
28	B322	65	M	F4	No virus	Yes	Two foci	Trabecular, inflammation	II
29	B326	54	M	F4	HCV GT 1b (5.18 log10)	Yes	Singular	Trabecular	III
30	B370	60	M	F0	No virus	Yes	Multifocal	Trabecular, focally clear cell	II
31	B399	52	M	F4	HCV GT 1b (4.23 log10)	Yes	Multifocal	Trabecular	III
32	B410	76	M	F4	No virus	Yes	Multifocal	Trabecular	II
33	B442	57	M	F4	No virus	Yes	Multifocal	Trabecular, lamellary fibrosis	III
34	B459	50	M	F4	HBV	No	Singular	Trabecular	II
35	B540	63	M	F4	No virus	Yes	Multifocal	Trabecular, inflammation, steatosis	II
36	B568	85	M	NA	No virus	Yes	Three foci	Trabecular, partly necrotic	II
37	B592	76	M	F4	No virus	Yes	Multifocal, diffuse	Trabecular, hyaline globules	II
38	B597	57	M	F4	No virus	Yes	Singular	Trabecular	II

HBV, hepatitis B virus.

← result is shown. Right panel shows enlargement of delimited areas. Chromatin condensation, an apoptotic nuclear feature, is clearly visible in C57BL6 mouse that received DEN. (D) Body weight, liver weight, number and size of macroscopic lesions recognizable from the outside were measured 40 weeks after DEN injection. Results are expressed as mean ± SEM from 22 control mice and 17 HCV transgenic animals. (E) Macroscopic and microscopic examples of liver tumors from C57BL6 and B6HCV mice 40 weeks after receiving 5 µg/g of DEN. Liver tumors were easily recognizable as spherical, light-brown nodules by macroscopy. Histology (H&E stain) showed round nodular formation of atypical liver cells compressing adjacent liver parenchyma consistent with murine liver cell adenoma.

confirmed these data on the protein level and showed that PP2Ac protein is more significantly upregulated in tumorous tissues than in non-tumorous surrounding tissues both from non-CHC-related HCC samples (Figure 6B). This upregulation was not visible in CHC-related HCC tissues because of the elevated expression level of PP2Ac in non-tumorous liver parenchyma in patients with CHC compared with control samples from patients with other liver diseases (30). Because of this increased expression of PP2Ac in non-tumorous tissues, we excluded CHC patients from the overall analysis. We then analyzed the expression of *Noxa* and *PUMA*, two p53-dependent genes that were altered by PP2A upregulation *in vitro*. Our data showed no significant difference of *Noxa* expression between tumorous and non-tumorous samples (Figure 6D). However, we observed a significant reduction of *PUMA* expression in malignant versus non-tumorous tissue (Figure 6C).

Discussion

We have reported previously that HCV-induced PP2Ac upregulation impairs epigenetic changes on histone H4 and inhibits DNA damage repair machinery (4,7). In the present study, we show that PP2Ac

also inhibits p53. As a consequence, B6HCV mice that overexpress PP2Ac in the liver have an increased susceptibility for HCC. We realize that our HCV-mediated PP2Ac overexpression mouse is an indirect *in vivo* model to experimentally explore the consequences of PP2Ac overexpression. A transgenic mouse model of PP2Ac overexpression would be preferable, but no such animal model is available. However, given our findings in cells with overexpression and silencing of PP2Ac, and the results in regard to serine phosphorylation of p53 and p53 target gene induction in the B6HCV animal model, we conclude that PP2A-induced dysregulation of p53 is an important mechanism of HCC carcinogenesis. Interestingly, in several experimental systems, PP2A has tumor suppressor functions (31). In our model, PP2A seems to predispose cells to transformation by altering p53 functions. There have been other reports of the procarcinogenic role of PP2A, notably in testicular germ cell tumors and for T-cell leukemia cells (32,33).

DEN is a well-known liver carcinogen (34). DEN is usually injected at doses 50–200 $\mu\text{g/g}$ of body weight to rats (35–37) and at doses 75–90 $\mu\text{g/g}$ of body weight to mice (38,39) to induce liver tumors. Some studies have used DEN at 5 $\mu\text{g/g}$ of body weight associated with a second injection of a liver tumor promoter, 2 weeks after DEN administration (40). At the dosages of 75–90 $\mu\text{g/g}$ of body weight, mice develop liver tumors by 40 weeks. Therefore, in order to test if HCV-mediated PP2Ac overexpression could predispose mice to liver tumors, we have deliberately injected a single low dose of 5 $\mu\text{g/g}$ of DEN. Our results show that B6HCV had a higher incidence of liver tumor formation than the control mice, presumably caused by an initial higher expression of PP2Ac that facilitates DNA damage and inhibits p53-mediated apoptosis.

The proapoptotic function of the tumor suppressor p53 is controlled by numerous posttranslational modifications on several residues. We have focused on some specific and characterized residues. It has been shown that PP2A inhibition or knocking down using pharmacological inhibitors or small interfering RNA, respectively, enhanced phosphorylation on serine 46 and induced apoptosis (41). Additionally, using PP2A inhibitors, it has been demonstrated that PP2A dephosphorylates serine 37 and negatively controls p53 transcriptional activity (19). In line with these previous observations, we show that PP2Ac overexpression impairs phosphorylation of p53 on serine 37 and 46 but not on serine 15. Our observation that etoposide-induced serine 15 phosphorylation is reduced only in UHCV57.3 cells is intriguing. However, it has been reported previously that phosphorylation on serine 15 can substantially be suppressed by a high expression of HCV core in HepG2 cells (42). Therefore, we hypothesize that the impairment of phosphorylation on serine 15 might be caused by a high expression of the core in these HCV-inducible cells independently of PP2Ac upregulation. Similarly, the reduction of serine 18 phosphorylation, a homolog of serine 15 in human, in HCV transgenic mice was presumably due to an elevated expression of HCV core in these animals. Surprisingly, we did not observe an impaired serine 15 phosphorylation in HCV-infected Huh7 cells. The discrepancy could be caused by a more restricted subcellular location or a lower expression level of HCV core protein during HCV replication in the infectious cell culture system compared with UHCV57.3 cells. Further analyses are required to clarify this issue.

It has been shown that p53 serine residues can be phosphorylated by a number of kinases, amongst them ATM, DNA-PK and p38MAPK (41,43,44). Therefore, PP2A might decrease serine 37 and 46 phosphorylation by regulating one or more of these kinases. However, the specific dephosphorylation of p53 serine 37 and 46 observed in the *in vitro* dephosphorylation assays (Supplementary Figure S2, available at *Carcinogenesis* Online) provides evidence for a direct mechanism where the phosphatase enzymatic activity of PP2A is responsible for the dephosphorylation of serine 37 and 46.

We have reported previously that PP2A catalytic subunit is overexpressed in liver biopsies from patients chronically infected with

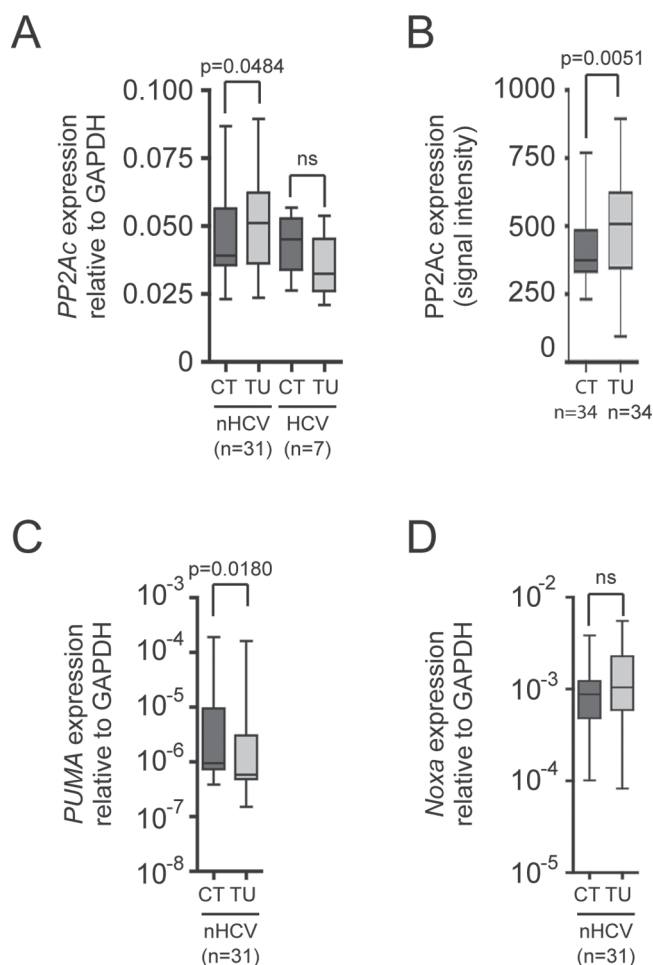


Fig. 6. PP2Ac is highly expressed in malignant tissues from non-CHC-related HCC and negatively correlates with *PUMA* expression. Quantitative reverse transcription-PCR was performed on paired liver biopsies (CT = non-malignant surrounding tissues; TU = malignant tissues) from CHC ($n = 7$) and non-CHC-derived HCC ($n = 31$). (A) PP2Ac expression level was determined in CHC and non-CHC samples. (B) PP2Ac protein expression level was evaluated by immunoblotting from non-CHC samples. (C) *PUMA* and (D) *Noxa* expression levels were measured in non-CHC samples. Results are shown as box plots, and statistical analysis was performed using Mann-Whitney's test.

HCV. Because our *in vitro* and *in vivo* data demonstrated that PP2A overexpression leads to impairment of p53-induced apoptosis and correlates with more HCC foci formation in the presence of mutagenic agents, we expected to measure a significantly higher expression of PP2Ac in tumorous biopsies than in non-tumorous biopsies from CHC-related HCC. Because of the elevated expression level of PP2Ac in non-tumorous liver parenchyma in patients with CHC compared with control samples from patients with other liver diseases (30), we were not able to measure a difference in the expression level between non-tumorous versus tumorous tissues. However, analysis of paired biopsies from non-CHC-derived HCC clearly showed an overexpression of PP2Ac in tumorous versus non-tumorous samples. The transcription factor, cyclic adenosine monophosphate response element-binding protein (CREB), is overexpressed or activated in several malignancies (45). For instance, total and active CREB is enhanced in HCC samples versus normal liver samples in a rat model of HCC (46). Furthermore, we have reported that endoplasmic reticulum stress response induces PP2Ac upregulation via CREB activation (5). Thus, we believe that the increased expression of PP2Ac in tumorous tissues from non-CHC related HCC is presumably caused by CREB transcriptional activity. Taken together, our data show an elevated expression of PP2Ac in tumorous samples and a negative correlation with *PUMA*, suggesting that PP2Ac upregulation provides favorable conditions for carcinogenesis.

In conclusion, we demonstrated that PP2Ac overexpression participates in tumor establishment and maintenance by altering the apoptotic cell death program. Importantly, this is the first report that associates HCV-induced PP2Ac overexpression with liver tumors.

Supplementary material

Supplementary Figures S1–S3 can be found at <http://carcin.oxfordjournals.org/>

Funding

Schweizerische Krebsliga (KLS-02522-02-2010); Swiss National Science Foundation (320030_130243); Forschungsfonds der Universität Basel (DMS2125).

Conflict of Interest Statement: None declared.

References

- Bosch, F.X. *et al.* (2004) Primary liver cancer: worldwide incidence and trends. *Gastroenterology*, **127** (5 suppl. 1), S5–S16.
- McGivern, D.R. *et al.* (2011) Virus-specific mechanisms of carcinogenesis in hepatitis C virus associated liver cancer. *Oncogene*, **30**, 1969–1983.
- Moriya, K. *et al.* (1998) The core protein of hepatitis C virus induces hepatocellular carcinoma in transgenic mice. *Nat. Med.*, **4**, 1065–1067.
- Duong, F.H. *et al.* (2004) Hepatitis C virus inhibits interferon signaling through up-regulation of protein phosphatase 2A. *Gastroenterology*, **126**, 263–277.
- Christen, V. *et al.* (2007) Activation of endoplasmic reticulum stress response by hepatitis viruses up-regulates protein phosphatase 2A. *Hepatology*, **46**, 558–565.
- Millward, T.A. *et al.* (1999) Regulation of protein kinase cascades by protein phosphatase 2A. *Trends Biochem. Sci.*, **24**, 186–191.
- Duong, F.H. *et al.* (2010) Hepatitis C virus-induced up-regulation of protein phosphatase 2A inhibits histone modification and DNA damage repair. *Hepatology*, **51**, 741–751.
- Branzei, D. *et al.* (2008) Regulation of DNA repair throughout the cell cycle. *Nat. Rev. Mol. Cell Biol.*, **9**, 297–308.
- Saretzki, G. (2010) Cellular senescence in the development and treatment of cancer. *Curr. Pharm. Des.*, **16**, 79–100.
- Van Hoof, C. *et al.* (2003) Phosphatases in apoptosis: to be or not to be, PP2A is in the heart of the question. *Biochim. Biophys. Acta*, **1640**, 97–104.
- Okamoto, K. *et al.* (2002) Cyclin G recruits PP2A to dephosphorylate Mdm2. *Mol. Cell*, **9**, 761–771.
- Amaral, J.D. *et al.* (2009) p53 and the regulation of hepatocyte apoptosis: implications for disease pathogenesis. *Trends Mol. Med.*, **15**, 531–541.
- Freed-Pastor, W.A. *et al.* (2012) Mutant p53: one name, many proteins. *Genes Dev.*, **26**, 1268–1286.
- Mallette, F.A. *et al.* (2007) The DNA damage signaling pathway connects oncogenic stress to cellular senescence. *Cell Cycle*, **6**, 1831–1836.
- Chernov, M.V. *et al.* (2001) Regulation of ubiquitination and degradation of p53 in unstressed cells through C-terminal phosphorylation. *J. Biol. Chem.*, **276**, 31819–31824.
- Puca, R. *et al.* (2010) Regulation of p53 activity by HIPK2: molecular mechanisms and therapeutic implications in human cancer cells. *Oncogene*, **29**, 4378–4387.
- Lavin, M.F. *et al.* (2006) The complexity of p53 stabilization and activation. *Cell Death Differ.*, **13**, 941–950.
- Ichwan, S.J. *et al.* (2006) Defect in serine 46 phosphorylation of p53 contributes to acquisition of p53 resistance in oral squamous cell carcinoma cells. *Oncogene*, **25**, 1216–1224.
- Li, D.W. *et al.* (2006) Protein serine/threonine phosphatase-1 dephosphorylates p53 at Ser-15 and Ser-37 to modulate its transcriptional and apoptotic activities. *Oncogene*, **25**, 3006–3022.
- Vogelstein, B. *et al.* (2000) Surfing the p53 network. *Nature*, **408**, 307–310.
- Vousden, K.H. *et al.* (2007) p53 in health and disease. *Nat. Rev. Mol. Cell Biol.*, **8**, 275–283.
- Sherr, C.J. *et al.* (2002) The RB and p53 pathways in cancer. *Cancer Cell*, **2**, 103–112.
- Moradpour, D. *et al.* (1998) Continuous human cell lines inducibly expressing hepatitis C virus structural and nonstructural proteins. *Hepatology*, **28**, 192–201.
- Pietschmann, T. *et al.* (2006) Construction and characterization of infectious intragenotypic and intergenotypic hepatitis C virus chimeras. *Proc. Natl Acad. Sci. USA*, **103**, 7408–7413.
- Blindenbacher, A. *et al.* (2003) Expression of hepatitis C virus proteins inhibits interferon alpha signaling in the liver of transgenic mice. *Gastroenterology*, **124**, 1465–1475.
- Sarasin-Filipowicz, M. *et al.* (2009) Alpha interferon induces long-lasting refractoriness of JAK-STAT signaling in the mouse liver through induction of USP18/UBP43. *Mol. Cell Biol.*, **29**, 4841–4851.
- Thoolen, B. *et al.* (2010) Proliferative and nonproliferative lesions of the rat and mouse hepatobiliary system. *Toxicol. Pathol.*, **38** (suppl. 7), 5S–81S.
- Chao, E.C. *et al.* (2006) Molecular models for the tissue specificity of DNA mismatch repair-deficient carcinogenesis. *Nucleic Acids Res.*, **34**, 840–852.
- Jang, J.J. *et al.* (1992) Progressive atypia in spontaneous and N-nitrosodiethylamine-induced hepatocellular adenomas of C3H/HeNcr mice. *Carcinogenesis*, **13**, 1541–1547.
- Duong, F.H. *et al.* (2006) S-Adenosylmethionine and betaine correct hepatitis C virus induced inhibition of interferon signaling *in vitro*. *Hepatology*, **43**, 796–806.
- Mumby, M. (2007) PP2A: unveiling a reluctant tumor suppressor. *Cell*, **130**, 21–24.
- Boudreau, R.T. *et al.* (2007) Apoptosis induced by protein phosphatase 2A (PP2A) inhibition in T leukemia cells is negatively regulated by PP2A-associated p38 mitogen-activated protein kinase. *Cell. Signal.*, **19**, 139–151.
- Schweyer, S. *et al.* (2007) Expression and function of protein phosphatase 2A in malignant testicular germ cell tumours. *J. Pathol.*, **213**, 72–81.
- Lim, I.K. (2003) Spectrum of molecular changes during hepatocarcinogenesis induced by DEN and other chemicals in Fisher 344 male rats [Mechanisms of Ageing and Development 123 (2002) 1665–1680]. *Mech. Ageing Dev.*, **124**, 697–708.
- Mukherjee, B. *et al.* (2005) Characterization of insulin-like-growth factor II (IGF II) mRNA positive hepatic altered foci and IGF II expression in hepatocellular carcinoma during diethylnitrosamine-induced hepatocarcinogenesis in rats. *J. Carcinog.*, **4**, 12.
- Pascale, R.M. *et al.* (2005) Role of HSP90, CDC37, and CRM1 as modulators of P16(INK4A) activity in rat liver carcinogenesis and human liver cancer. *Hepatology*, **42**, 1310–1319.
- Schiffer, E. *et al.* (2005) Gefitinib, an EGFR inhibitor, prevents hepatocellular carcinoma development in the rat liver with cirrhosis. *Hepatology*, **41**, 307–314.
- Yamamoto, Y. *et al.* (2004) The orphan nuclear receptor constitutive active/androstane receptor is essential for liver tumor promotion by phenobarbital in mice. *Cancer Res.*, **64**, 7197–7200.
- Yoshiji, H. *et al.* (2004) Halting the interaction between vascular endothelial growth factor and its receptors attenuates liver carcinogenesis in mice. *Hepatology*, **39**, 1517–1524.

40. Kalinichenko, V.V. *et al.* (2004) Foxm1b transcription factor is essential for development of hepatocellular carcinomas and is negatively regulated by the p19ARF tumor suppressor. *Genes Dev.*, **18**, 830–850.
41. Saito, S. *et al.* (2002) ATM mediates phosphorylation at multiple p53 sites, including Ser(46), in response to ionizing radiation. *J. Biol. Chem.*, **277**, 12491–12494.
42. Kao, C.F. *et al.* (2004) Modulation of p53 transcription regulatory activity and post-translational modification by hepatitis C virus core protein. *Oncogene*, **23**, 2472–2483.
43. Tibbetts, R.S. *et al.* (1999) A role for ATR in the DNA damage-induced phosphorylation of p53. *Genes Dev.*, **13**, 152–157.
44. Perfettini, J.L. *et al.* (2005) Essential role of p53 phosphorylation by p38 MAPK in apoptosis induction by the HIV-1 envelope. *J. Exp. Med.*, **201**, 279–289.
45. Conkright, M.D. *et al.* (2005) CREB: the unindicted cancer co-conspirator. *Trends Cell Biol.*, **15**, 457–459.
46. Kovach, S.J. *et al.* (2006) Role of cyclic-AMP responsive element binding (CREB) proteins in cell proliferation in a rat model of hepatocellular carcinoma. *J. Cell. Physiol.*, **206**, 411–419.

Received January 7, 2013; revised June 20, 2013; accepted July 7, 2013